5G NR Support for UAV-Assisted Cellular Communication on Non-Terrestrial Network

Justine Cris Borromeo
Instituto di Telecommunicazione, Informatica e Fotonica
Scuola Superiore Sant'Anna
Pisa, Italy
justinecris.borromeo@santannapisa.it

Koteswararao Kondepu
Department of Computer Science and Engineering
Indian Institute of Technology Dharwad
Dharwad, India
k.kondepu@iitdh.ac.in

Nicola Andriolli
Institute of Electronics, Information Engineering and Telecommunications
National Research Council of Italy
Pisa, Italy
nicola.andriolli@ieiit.cnr.it

Luca Valcarenghi
Instituto di Telecommunicazione, Informatica e Fotonica
Scuola Superiore Sant'Anna
Pisa, Italy
l.valcarenghi@santannapisa.it

Riccardo Bassoli
Deutsche Telekom Chair of Communication Networks
Technische Universität Dresden
Dresden, Germany
riccardo.bassoli@tu-dresden.de

Frank H.P. Fitzek
Deutsche Telekom Chair of Communication Networks
Technische Universität Dresden
Dresden, Germany
frank.fitzek@tu-dresden.de

***Abstract*—The use of Unmanned Aerial Vehicles (UAVs) to provide cellular communication in rural areas, disaster-hit regions, or during temporary events is gaining increasing attention due to its flexible deployment and energy efficiency compared to fixed terrestrial infrastructures. However, UAVs experience significant challenges such as the limited wireless connectivity provided by *Ka-band* frequency, and their flying time is constrained by the energy consumed during the data transmission and the complexity of the Baseband Unit (BBU) implementation. Using different lower layer functional split options (e.g., 7-1, 7-2, 7-2x, and 7-3), this paper provides a theoretical and simulation analysis of the 5G New Radio (NR) physical layer specifications to achieve a fronthaul bandwidth that can be supported by the *Ka-band*. These functional split options are then compared in terms of fronthaul bandwidth, theoretical throughput, connection density, number of functions deployed at the UAV, and the energy consumption of the fronthaul transmission to determine which functional split option is better suited for a multi-layered Non-Terrestrial Network (NTN).**

***Index Terms*—Non-terrestrial network, unmanned aerial vehicle, wireless communications, 5G new radio.**

I. Introduction

Until the rise of 5G, Non-Terrestrial Networks (NTNs) are generally provided by stand-alone satellites operating on Low Earth Orbits (LEO), Medium Earth Orbits (MEO) or Geostationary Earth Orbits (GEO), which mainly support services like navigation, TV broadcasting, and meteorology. With the evolution of 5G and beyond, NTNs are exploited to improve the limited performance of 5G terrestrial networks specifically in unserved/underserved areas, disaster hit regions where the terrestrial networks are in outage, or in hotspot areas where terrestrial infrastructures are overloaded [1], [2].

Satellites offer extremely large coverage regions and favorable line of sight connectivity, however, they also suffer from severe path loss (PL), long communication delays, and expensive installations costs [3]. Thus, multilayered hierarchical NTNs, comprising of Satellites, Low Altitude Platforms (LAPs), and High Altitude Platforms (HAPs) have been explored with the support of 5G New Radio (NR) to realize a cost-effective solution to provide continuous, resilient and ubiquitous wireless coverage, and enable network scalability making them more suitable in future networks, and emergency communications [4], [5].

Recently, the use of LAPs such as Unmanned Aerial Vehicles (UAVs) to provide broadband wireless connectivity on rural areas, during disasters or temporary events, and to relay services for terrestrial mobile nodes has been gaining increasing attention since they can be deployed on demand making them more energy efficient compared to always-on fixed terrestrial infrastructures [6]. However, significant challenges arise when integrating UAV into a multi-layered NTN because of its limited power supply.

The first concern is when running Baseband Unit (BBU) functions in the UAV due to its complex implementation [7]. Increasing the complexity of functions deployed in the UAV also increases its energy consumption, resulting to a shorter flying time since UAVs are battery powered. To reduce the computational complexity, lower layer functional splits are considered (e.g., 7-1, 7-2, 7-2x and 7-3) where Radio Unit (RU) functions are implemented in the UAV.

Another concern is that UAV should also support the transmission and reception of data in the fronthaul interface between UAV and the satellite which performs other 5G BBU functions. 3GPP defined the fronthaul bandwidth and latency requirements of different functional split options [8], [9]. Using lower layer split, the fronthaul bandwidth in the downlink direction is around $9.8Gbps$ for option 7-1, while $10.1Gbps$ for options 7-2, 7-2x and 7-3. To achieve this bandwidth, operation in millimeter wave (mm-wave) is being considered for an integrated nanosatellite-5G system [10] with some configurations and trade-offs discussed in [11]. However, there are still open challenges when using mm-wave, such as channel modeling considering the impact of Doppler effect, fading, and multipath components, which is challenging at higher frequencies. Thus, this research will focus on using the current satellite communication frequency bands (e.g., S-, and Ka-band) and adjust the 5G physical layer specifications to achieve a fronthaul bandwidth that can be supported by the S- or Ka-band. Using satellite communication frequency bands, which are the S-band at $2GHz$ and the Ka-band at $20GHz$, multi-layered NTN have been evaluated in [2]. Based on their results, more than $0.3Gbps$ in the former and $3Gbps$ in the latter can be achieved when a GEO layer is assisted by HAPs operating in the stratosphere. Thus, this research will focus on the analysis of a multi-layered NTN using the Ka-band frequency.

With the results obtained in [2], this research shows a theoretical and simulation analysis on implementing a UAV as RU in a multi-layered NTN. First, we evaluate and analyze different physical layer specifications to achieve a fronthaul bandwidth that can be supported by the *Ka-band*. Then, we compare four different lower layer functional split options (7-1, 7-2, 7-2x and 7-3) in terms of fronthaul bandwidth, theoretical throughput, connection density, energy consumption for fronthaul transmission, and the number of functions implemented in the RU to determine which functional split option can be considered in a multi-layered NTN scenario.

II. 5G NR on Non-Terrestrial Network (NTN)

NTNs refer to segments of networks operating through space or air vehicles to provide wireless communication. As shown in Fig. 1, different types of NTN platforms are considered:

- Geostationary Earth Orbits (GEO) satellites have a circular orbit on the Earth's equatorial plane at an altitude of $35800km$. GEO are continuously visible from terrestrial terminals and can cover a very large geographical area. However, they experience a very large propagation delay and attenuation because of their high altitude from the earth.
- Medium Earth Orbits (MEO) satellites have a circular orbit around the Earth at an altitude between $7000km$ and $25000km$. With their altitude lower than GEO, MEOs can have better signal strength and lower propagation delay compared to the GEO. However, they are non-stationary and must operate in a constellation to maintain service continuity.
- Low Earth Orbits (LEO) satellites have a circular orbit around the Earth with varying altitude from $300km$ to $1500km$. LEO satellites are also non-stationary and can have better signal strength and lower propagation delay than the GEO and the MEO. However, they can cover a smaller geographical area compared to the GEO and MEO.
- High Altitude Platforms (HAPs) like hot-air balloons or airships are deployed in the stratosphere at an altitude of around $20km$. HAPs are considered to support a more cost-effective services and flexible deployment than the satellites.
- Low Altitude Platforms (LAPs) like UAVs fly with an altitude of around $100m$. They provide significant performance improvement compared to HAPs thanks to their low altitude deployment and sort range line-of-sight communication. They also allow a cheaper and faster deployment than HAPs. UAVs on the other hand poses power constraints due to a limited power supply.

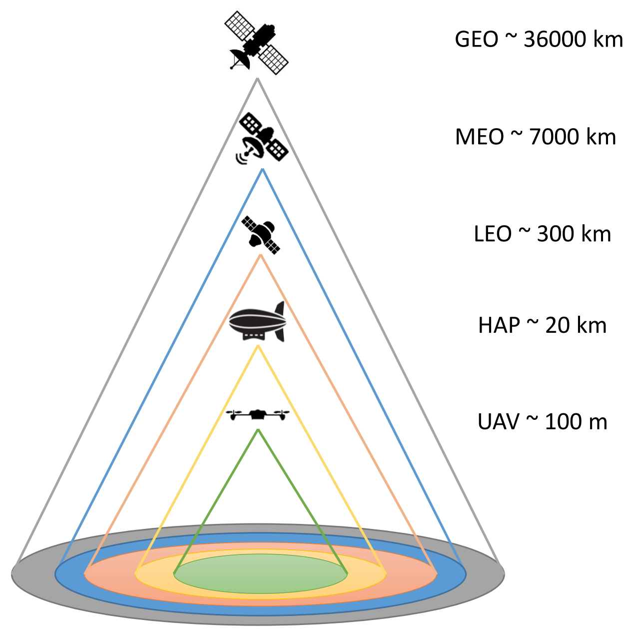

Fig. 1. Different types of non-terrestrial network stations.

Satellite communication offers some advantages to ground user as they provide large coverage area, and line-of-sight connectivity. However, they also suffer from severe path loss and huge communication delays, which is critical in 5G NR. To improve the performance of stand-alone satellite communications and provide better coverage, flexibility, and resilience, multi-layered hierarchical networks have been proposed [12].

Multi-layered satellite networks are realized by integrating satellite and aerial networks, and are characterized by a hierarchical structure [13]. In this scenario, the wireless communication performance can be improved when complementing satellite communication systems with aerial networks like HAPs and LAPs. A recent study in [2] shows that GEO-HAP-Earth multi-layered configuration can best bridge satellite signals to the ground with $6x$ better capacity than a point-to-point GEO transmission. In this research, we consider having UAV on the aerial network to compliment with the satellite network due to its cheap and fast deployment.

This paper focuses on the multi-layered heterogeneous platforms where the Distributed Unit (DU) and Central Unit (CU) functions are implemented in the satellite (GEO, MEO or LEO), while RU functions are deployed in the UAV using lower layer splits.

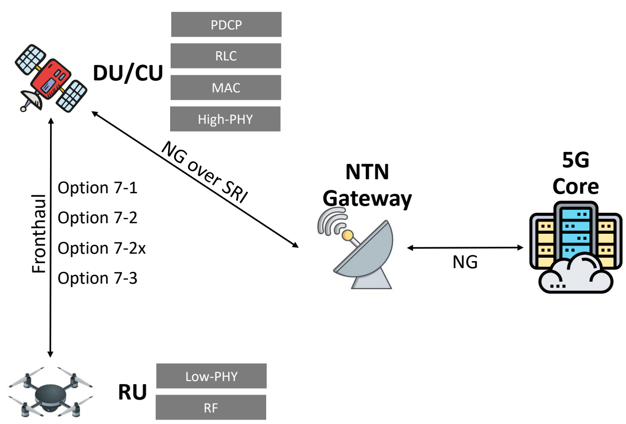

Fig. 2. Multi-layered NTN overview.

Fig. 2 shows the overview of the multi-layered NTN where the 5G core network is connected to the satellite through an NTN gateway using the NG Satellite Radio Interface (SRI), and the satellite is connected to the UAV via the fronthaul interface.

III. Performance Parameters

Five different performance parameters are considered to analyze the 5G NR support for a satellite-UAV multi-layered NTN scenario, namely: fronthaul bandwidth, theoretical throughput, connection density, number of functions implemented in the UAV, and the energy consumed in receiving the fronthaul data in the downlink direction. This section describes each of these parameters and discusses physical layer functions that can be adjusted to support satellite-UAV communication, and still provide a good Quality of Service (QoS).

A. Fronthaul Bandwidth

Fronthaul bandwidth is the data rate that can be transferred between the RU and the DU. Based on [8], [14], the fronthaul bandwidth for option 7-1 can be computed using:

$$FH = N_{SC} * N_{SY} * N_{AP} * N_{BTW} * 2 * 1000 + MAC \quad (1)$$

while the fronthaul bandwidth for options 7-3, 7-2 and 7-2x can be determined using the formula below:

$$FH = N_{SC} * N_{SY} * N_{LA} * N_{BTW} * 2 * 1000 + MAC \quad (2)$$

- N_{SC} - number of subcarriers of each OFDM symbol
- N_{SY} - number of OFDM symbols in a subframe
- N_{LA} - number of layers
- N_{AP} - number of antenna ports
- N_{BTW} - IQ bitwidth
- MAC - MAC layer information

The number of subcarriers depends on the channel bandwidth used for transmission, while the subcarrier spacing determines the number of OFDM symbols in each subframe. The IQ bitwidth is considered to have 16-bits, and the MAC layer information is assumed to consume $121 Mbps$ for 7-1, and $713.9 Mbps$ for 7-2, 7-2x, and 7-3 [14].

The fronthaul bandwidth reported in [9] ($9.8 Gbps$ for option 7-1, while $10.1 Gbps$ for options 7-2, 7-2x and 7-3) is based on a scenario using $100 MHz$ (3276 subcarriers and 28 OFDM symbols), 8 layers and 32 antenna ports, which can be achievable when optical fiber is used in the fronthaul interface. Since the transmission between the satellite and the UAV is through a wireless channel, the required fronthaul bandwidth in [9] is difficult to achieve due to the limited capacity of the wireless technology currently used for satellite communication (*Ka-band*). To achieve the fronthaul bandwidth that can be supported by the *Ka-band*, physical layer specifications are modified (e.g., N_{SC}, N_{SY}, N_{LA}, and N_{AP}).

Simulations using 5G toolbox is also done to measure Physical Downlink Shared Channel (PDSCH) throughput of a 5G NR link [15]. This simulation provides the effect of the Signal-to-Noise Ratio (SNR), channel bandwidth, number of layers, and number of antenna ports to the throughput of the 5G NR link.

B. Theoretical Throughput

The throughput is measured as the information that the system can process in a given amount of time. According to 3GPP [16], the maximum data rate for a given number of aggregated carriers in a band or band combination can be computed using:

$$Throughput(Mbps) = 10^6 * \sum_{j=1}^{J} N_{LA}^j * Q_m^j * f^j * R_{max} * \frac{N_{SC}^j * N_{SY}^j}{T_s^\mu} * (1 - OH^j) \quad (3)$$

- J - number of aggregated component carriers
- N_{LA} - number of layers
- Q_m - maximum modulation order
- f - scaling factor where values can be taken from 0, 0.8, 0.75 or 0.4.
- R_{max} - code rate $= 948/1024$
- N_{SC} - number of subcarriers of each OFDM symbol
- N_{SY} - number of OFDM symbols in a subframe
- T_s^μ - time duration of each subframe in seconds
- OH - overhead which takes the following values: $[0.14]$ for FR1 frequency range in DL;$[0.18]$ for FR2 frequency range in DL; $[0.08]$ for FR1 frequency range in UL and; $[0.10]$ for FR2 frequency range in UL

Based on the specifications achieved in Section III-A, we can compute for the maximum cell throughput than can be provided to the end users using the formula above.

C. Connection Density

Connection density refers to the average number of user/devices that can be connected to the UAV. This can be achieved by dividing the theoretical cell throughput to the average user throughput. According to [17], the user experience throughput in a Average Revenue per User (ARPU) area is around $10Mbps$, and $50Mbps$ for rural areas. This will be our basis for computing for the connection density in the next section.

D. Number of Functions

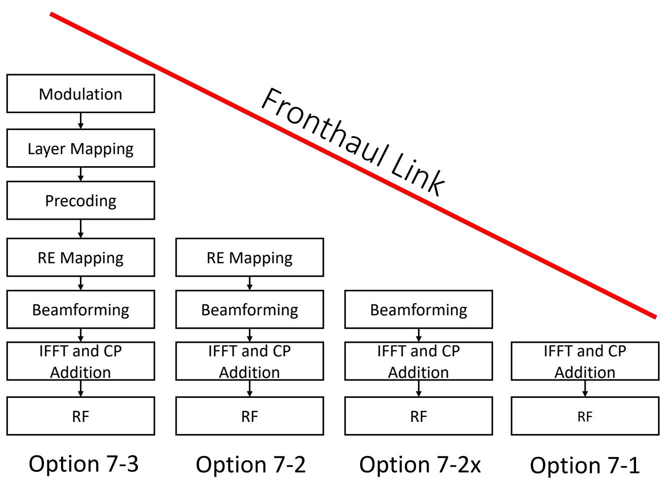

Fig. 3. Number of functions implemented in the RU using different lower layer split options.

Since the flying time of UAV is crucial in this multi-layered NTN platform, it is very important to determine the number of functions deployed in the UAV since it is proportional to its computational load and energy consumption. Fig. 3 shows the functions that is implemented in the UAV using different lower layer split options.

E. Energy Consumption (Fronthaul Connection)

The energy consumption of the data reception on the fronthaul interface is measured in terms of energy per bit (E_b), which is the signal power over the user bit rate, as shown in Eqn. 4 below:

$$E_b = P_R/R_B \tag{4}$$

- E_b - Energy per bit
- P_R - Received Power
- R_B - Bitrate

where the received power can be achieved using:

$$P_R = EIRP + G_R - Losses \tag{5}$$

- $EIRP$ - Equivalent Isotropic Radiated Power
- G_R - Receiver gain
- Losses in the signal can be due to free space path loss (FSPL), atmospheric loss (AL), and scintillation loss (SL)

Typical values of $EIRP$, G_R, and losses are defined in [5] and [18] where $EIRP = 66dBW$, $G_R = 35.3dBi$, $FSPL = 184.6dB$, $AL = 0.5dB$, and $SL = 0.3dB$.

IV. Result

This section shows some theoretical and simulation results on the key performance parameters discussed in Section III. Some physical layer specifications are modified to achieve the required data rate for multi-layered NTN in the *Ka-band*, which is discussed in [2]. The aim is to achieve a fronthaul bandwidth from 3 to $6Gbps$ and analyze its effect on other parameters specifically on theoretical throughput and connection density. After achieving the desired fronthaul bandwidth, different lower layer functional split options (7-1, 7-2, 7-2x, 7-3) are compared to identify which split is best suited for multi-layered NTN scenario.

A. Fronthaul Bandwidth

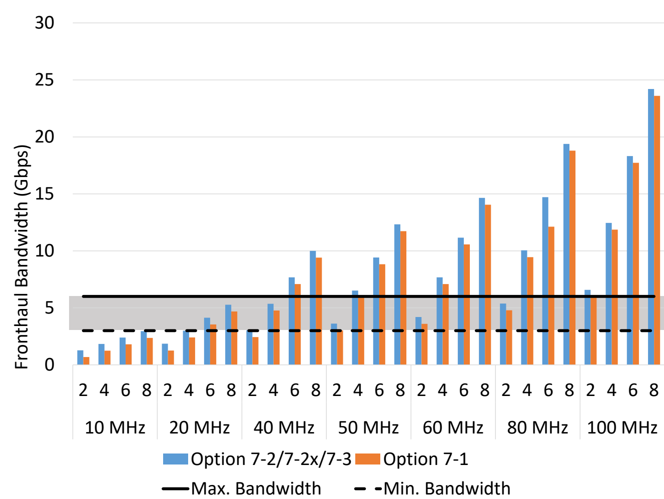

Fig. 4. Fronthaul bandwidth with varying channel bandwidth, number of layers, and number of antenna ports.

Fig. 4 shows the fronthaul bandwidth of different functional split options with varying channel bandwidth, and number of layers on FR1 frequency range (10 to $100MHz$). As shown in the figure, the fronthaul bandwidth increases with the increasing channel bandwidth and the number of layers.

Since we are looking into the fronthaul bandwidth that can possibly be supported by the *Ka-band*, a minimum and maximum bandwidth limit is considered and PHY layer specifications are varied to achieve a fronthaul bandwidth within this limit. In this case, we are specifically considering the following physical layer specifications: $80MHz$ with 2 layers; $40MHz$ with 4 layers; and $20MHz$ with 8 layers.

Results achieved in Fig. 4 only show the fronthaul bandwidth without considering the number of antenna ports used to

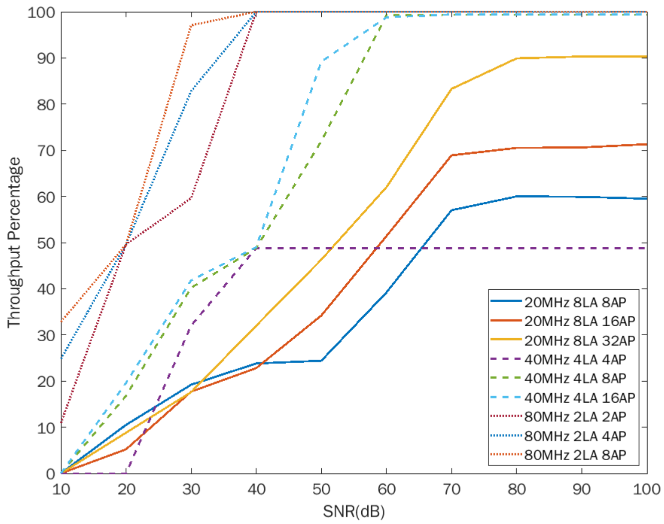

Fig. 5. Throughput percentage of different physical layer implementation with increasing SNR.

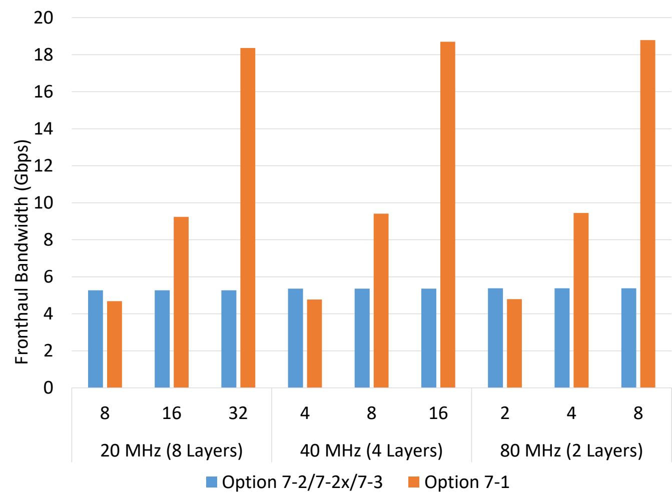

Fig. 6. Fronthaul bandwidth of 20MHz on 8 layers, 40MHz on 4 layers, and 80MHz on 2 layers with varying number of antenna ports.

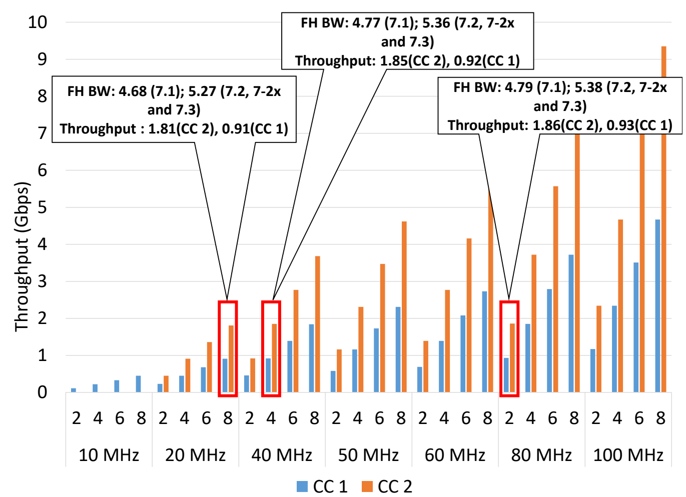

Fig. 7. Theoretical throughput with varying channel bandwidth and number of layers.

transmit to the end devices. The number of antenna ports also affects the throughput and quality of communication between UAV and end devices. To achieve the maximum throughput, a combination of higher SNR, lower number of layers, higher number of antennas should be considered.

To test the quality of transmission, simulations were done using the 5G toolbox [15]. Fig. 5 shows the throughput percentage of different physical layer specifications with increasing SNR. As shown in the figure, the throughput percentage increases together with the number of antennas. It can also be observed in the figure that a combination of a higher channel bandwidth and lower number of layers can achieve a higher throughput percentage (100% for $80MHz$ and $2LA$ at $40SNR$) compared to specifications with lower channel bandwidth and higher number of layers. Finally, it shows in the figure that using $80MHz$ channel bandwidth with 2 layers and 8 antenna ports can achieve the most throughput percentage even with a lower SNR.

Based from the graph achieved in Fig. 5, Fig. 6 shows the fronthaul bandwidth with $20MHz$ and 8 layers, $40MHz$ and 4 layers, and $80MHz$ and 2 layers while varying number of antenna ports. Since the fronthaul bandwidth for options 7-2, 7-2x, and 7-3 are not dependent on the number of antenna ports, it can be shown that the fronthaul bandwidth is constant while increasing the number of antenna ports. However, the fronthaul bandwidth for option 7-1 doubles when doubling the number of antenna ports, and the fronthaul bandwidth when $N_{AP} \geq 2 * N_{LA}$ can't be supported by the *Ka-band*.

B. Theoretical Throughput and Connection Density

This subsection shows the theoretical throughput to be provided to the end devices. Fig. 7 shows the theoretical throughput with varying channel bandwidth, number of layers, and number of component carriers. Based on the fronthaul bandwidth results from Section III-A, we can achieve a maximum theoretical throughput of $0.91 - 0.93Gbps$ when using 1 component carrier (CC1) while $1.81 - 1.86Gbps$ with 2 component carriers (CC2).

Considering a use case scenario in ARPU areas where the average user throughput is $10Mbps$, the multi-layered NTN can support around $91 - 93$ users with CC1 and $181 - 186$ users with CC2.

C. Overall Performance

This subsection shows which functional split option is better suited for multi-layered NTN. Four physical layer split options are being compared with regards to the performance parameters discussed in Section III. Based on the results achieved in Section IV-A, the comparison is based on the following physical layer specifications:

- $J = 2$

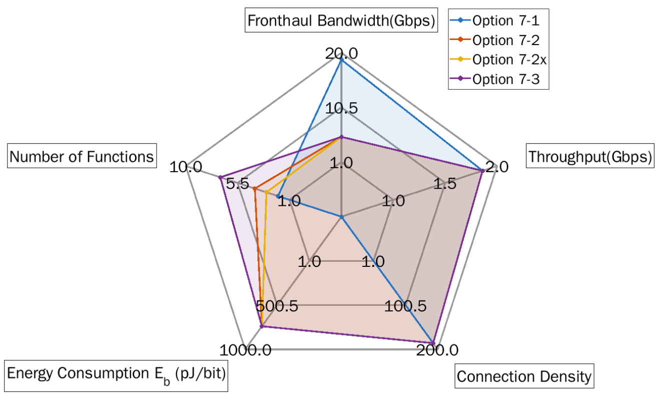

Fig. 8. Overall comparison of different physical layer functional split options.

- $Q_m = 256QAM$
- $N_{SC} = 217$ with $30kHz$ subcarrier spacing ($80MHz$ Channel Bandwidth)
- $N_{LA} = 2$
- $N_{AP} = 8$

Fig. 8 shows the comparison of four different functional split options in terms of fronthaul bandwidth, theoretical throughput, connection density, energy per bit, and number of functions implemented in the UAV. As shown in the figure, all functional split options provide the same throughput and connection density. However, option 7-1 requires more fronthaul bandwidth ($18.79Gbps$) to provide the same throughput compared to the others ($5.38Gbps$). Since the fronthaul bandwidth for option 7-1 is not support by the *Ka-band* frequency, the transmission energy consumption is only measured for options 7-2, 7-2x, and 7-3. Based on the equation provided in Section III-E, the energy per bit consumed on the fronthaul when using these split options is around $E_b = 739pJ/bit$. As for the number of functions that will be deployed in the UAV, it shows from Fig. 3 that option 7-1 has the least functions while option 7-3 has the most functions to be deployed in the UAV.

After comparing 4 physical layer functional split options, it shows that using option $7-2x$ is the most optimal solution on multi-layered NTN. It has the same results with option 7-2 and 7-3 in terms of fronthaul bandwidth, throughput, connection density and energy consumption, but with lesser number of functions in the UAV. Also, option 7-1 has a really high fronthaul bandwidth that cannot be supported by the *Ka-band* even if it has lesser number of functions in the UAV compared to option 7-2x.

V. Conclusion and Future Work

This paper analyzed the possibility of the 5G NR support for multi-layered NTN scenario. With the limited capacity of wireless communication on NTN, theoretical and simulation analysis are done to determine which physical layer specifications achieve a fronthaul bandwidth that can be supported by the *Ka-band* frequency. Results shown that 5G NR physical layer with $256QAM$ modulation, $80MHz$ channel bandwidth with 2 component carriers, 2 layers, and 8 antenna ports is the most ideal specification for multi-layered NTN. Using these specifications, we compared different functional split options in the physical layer in terms of fronthaul bandwidth, throughput, connections density, energy consumption and number of functions implemented in the UAV. Unfortunately, the fronthaul bandwidth provided by option 7-1 is too high and cannot be supported by the *Ka-band*. Results also shown that using option 7-2x for multi-layered NTN can achieve lesser number of functions compared to option 7-2 and 7-3.

Future work includes analyzing the 5G NR support on other satellite frequency bands (S-, C-, X-, and Ku band). Also, considering a 7-2x functional split, an OpenCL-based implementation of the Low-PHY in an FPGA System-on-Chip (SOCs) to be deployed in the UAV will be also considered.

Acknowledgment

This work was supported by the German Research Foundation (DFG, Deutsche Forschungsgemeinschaft) as part of Germany's Excellence Strategy—EXC 2050/1—Cluster of Excellence "Centre for Tactile Internet with Human-in-the-Loop" (CeTI) of Technische Universität Dresden under Project ID 390696704 and the Federal Ministry of Education and Research of Germany in the programme of "Souverän. Digital. Vernetzt." Joint project 6G-life, project identification number: 16KISK001K. This work has also been partially funded by the European Commission through the H2020 project Hexa-X (Grant Agreement no. 101015956). This work also received funding from the ECSEL JU grant agreement No 876967. The JU receives support from the EU Horizon 2020 research and innovation programme and the Italian Ministry of Education, University, and Research (MIUR). This work is also partly supported through a Faculty Fellowship awarded by DST NMICPS TiHAN at IIT Hyderabad and SERB Startup Research Grant (SRG-2021-001522).

References

[1] J. Liu, Y. Shi, Z. M. Fadlullah, and N. Kato, "Space-Air-Ground Integrated Network: A Survey," *IEEE Communications Surveys Tutorials*, vol. 20, no. 4, pp. 2714–2741, 2018.

[2] D. Wang, M. Giordani, M.-S. Alouini, and M. Zorzi, "The Potential of Multilayered Hierarchical Nonterrestrial Networks for 6G: A Comparative Analysis Among Networking Architectures," *IEEE Vehicular Technology Magazine*, vol. 16, no. 3, pp. 99–107, 2021.

[3] E. Cianca, R. Prasad, M. De Sanctis, A. De Luise, M. Antonini, D. Teotino, and M. Ruggieri, "Integrated satellite-HAP systems," *IEEE Communications Magazine*, vol. 43, no. 12, pp. supl.33–supl.39, 2005.

[4] M. M. Azari, S. Solanki, S. Chatzinotas, O. Kodheli, H. Sallouha, A. Colpaert, J. F. M. Montoya, S. Pollin, A. R. Haqiqatnejad, A. Mostaani, E. Lagunas, and B. E. Ottersten, "Evolution of Non-Terrestrial Networks From 5G to 6G: A Survey," *ArXiv*, vol. abs/2107.06881, 2021.

[5] 3rd generation Partnership Project:, "Technical Specification Group Radio Access Network; Solutions for NR to support non-terrestrial networks (NTN)," 3GPP, Technical Report (TR) 38.821, Mar. 2021, version 2.0.0.

[6] M. Giordani and M. Zorzi, "Non-Terrestrial Networks in the 6G Era: Challenges and Opportunities," *IEEE Network*, vol. 35, no. 2, pp. 244–251, 2021.

[7] R. Bassoli, F. Granelli, C. Sacchi, S. Bonafini, and F. H. Fitzek, “CubeSat-Based 5G Cloud Radio Access Networks: A Novel Paradigm for On-Demand Anytime/Anywhere Connectivity,” *IEEE Vehicular Technology Magazine*, vol. 15, no. 2, pp. 39–47, 2020.

[8] NTT DOCOMO:, “CU-DU split: Refinement for Annex A (Transport Network and RAN internal functional split),” 3GPP, Technical Report (TR) R3-162102, Oct. 2016.

[9] “Huber Suhner Functional Split,” https://www.hubersuhner.com/en/documents-repository/technologies/pdf/fiber-optics-documents/5g-fundamentals-functional-split-overview, last accessed: 2022-01-10.

[10] F. Babich, M. Comisso, A. Cuttin, M. Marchese, and F. Patrone, “Nanosatellite-5G Integration in the Millimeter Wave Domain: A Full Top-Down Approach,” *IEEE Transactions on Mobile Computing*, vol. 19, no. 2, pp. 390–404, 2020.

[11] M. Giordani and M. Zorzi, “Satellite Communication at Millimeter Waves: a Key Enabler of the 6G Era,” in *2020 International Conference on Computing, Networking and Communications (ICNC)*, 2020, pp. 383–388.

[12] J. Liu, Y. Shi, Z. M. Fadlullah, and N. Kato, “Space-air-ground integrated network: A survey,” *IEEE Communications Surveys & Tutorials*, vol. 20, no. 4, pp. 2714–2741, 2018.

[13] H. Nishiyama, Y. Tada, N. Kato, N. Yoshimura, M. Toyoshima, and N. Kadowaki, “Toward optimized traffic distribution for efficient network capacity utilization in two-layered satellite networks,” *IEEE Transactions on Vehicular Technology*, vol. 62, no. 3, pp. 1303–1313, 2013.

[14] CMCC, “Transport requirement for CU & DU functional split options,” 3GPP, Technical Report (TR) R3-161813, Aug. 2016.

[15] “5G Toolbox: 5G NR PDSCH Throughput,” https://de.mathworks.com/help/5g/ug/nr-pdsch-throughput.html, last accessed: 2022-05-05.

[16] 3rd generation Partnership Project:, “User Equipment (UE) Radio Access Capabilities,” 3GPP, Technical Report (TR) 38.306, Sep. 2018, version 15.2.0.

[17] NMGN Alliance, “NMGN 5G White Paper,” NMGN, White Paper, Feb. 2015.

[18] ITU-R, “Deployment and technical characteristics of broadband high altitude platform stations in the fixed service in the frequency bands 6440-6520 MHz, 21.4-22.0 GHz, 24.25-27.5 GHz, 27.9-28.2 GHz, 31.0-31.3 GHz, 38.0-39.5 GHz, 47.2-47.5 GHz and 47.9-48.2 GHz used in sharing and compatibility studies,” ITU-R, Technical Report (TR) F.2439-0, Nov. 2018.